ADVANCED FUNCTIONAL MATERIALS
www.afm-journal.de

Tissue Adhesive Catechol-Modified Hyaluronic Acid Hydrogel for Effective, Minimally Invasive Cell Therapy

*Jisoo Shin, Jung Seung Lee, Changhyun Lee, Hyun-Ji Park, Kisuk Yang, Yoonhee Jin, Ji Hyun Ryu, Ki Sung Hong, Sung-Hwan Moon, Hyung-Min Chung, Hee Seok Yang, Soong Ho Um, Jong-Won Oh, Dong-Ik Kim, Haeshin Lee, and Seung-Woo Cho**

Current hyaluronic acid (HA) hydrogel systems often cause cytotoxicity to encapsulated cells and lack the adhesive property required for effective localization of transplanted cells in vivo. In addition, the injection of hydrogel into certain organs (e.g., liver, heart) induces tissue damage and hemorrhage. In this study, we describe a bioinspired, tissue-adhesive hydrogel that overcomes the limitations of current HA hydrogels through its improved biocompatibility and potential for minimally invasive cell transplantation. HA functionalized with an adhesive catecholamine motif of mussel foot protein forms HA-catechol (HA-CA) hydrogel via oxidative crosslinking. HA-CA hydrogel increases viability, reduces apoptosis, and enhances the function of two types of cells (human adipose-derived stem cells and hepatocytes) compared with a typical HA hydrogel crosslinked by photopolymerization. Due to the strong tissue adhesiveness of the HA-CA hydrogel, cells are easily and efficiently transplanted onto various tissues (e.g., liver and heart) without the need for injection. Stem cell therapy using the HA-CA hydrogel increases angiogenesis in vivo, leading to improved treatment of ischemic diseases. HA-CA hydrogel also improved hepatic functions of transplanted hepatocytes in vivo. Thus, this bioinspired, tissue-adhesive HA hydrogel can enhance the efficacy of minimally invasive cell therapy.

1. Introduction

Hyaluronic acid (HA) hydrogels have been explored as scaffold materials for cell therapy and tissue engineering. HA is interactive and binds to various types of cells due to the presence of cell surface receptors for HA (e.g., CD44, ICAM-1, and RHAMM), through which HA increases cell-matrix interaction and initiates signal transduction essential for cell survival and function.[1–3] HA is also easily functionalized with various crosslinking moieties via its carboxyl or hydroxyl group to produce 3D hydrogel.[1,2] Due to these advantageous properties, HA has been applied as a desirable hydrogel material for the culture and transplantation of a wide variety of cells, including chondrocytes, osteoblasts, endothelial cells, and stem cells.[1,2,4,5]

HA hydrogels have typically been prepared by chemical and physical crosslinking of HA conjugate modified with several functional groups

J. Shin, J. S. Lee, C. Lee, H.-J. Park, K. Yang, Dr. Y. Jin, Prof. J.-W. Oh, Prof. S.-W. Cho
Department of Biotechnology
Yonsei University
50 Yonsei-ro, Seodaemun-gu, Seoul 120-749, South Korea
E-mail: seungwoocho@yonsei.ac.kr
Dr. J. H. Ryu, Prof. H. Lee
The Graduate School of Nanoscience and Technology
Department of Chemistry
Korea Advanced Institute of Science and Technology
291 Daehak-ro, Yuseong-gu, Daejeon 305-701, South Korea
K. S. Hong, Prof. S.-H. Moon, Prof. H.-M. Chung
Department of Stem Cell Biology
Konkuk University School of Medicine
120 Neungdong-ro, Gwangjin-gu, Seoul 143-701, South Korea
Prof. H. S. Yang
Department of Nanobiomedical Science and BK21 PLUS NBM Global Research Center for Regenerative Medicine
Dankook University
119 Dandae-ro, Dongnam-gu, Cheonan 330-714, South Korea
Prof. S. H. Um
School of Chemical Engineering and SKKU Advanced Institute of Nanotechnology (SAINT)
Sungkyunkwan University
2066 Seobu-ro, Jangan-gu, Suwon 440-746, South Korea
Prof. D.-I. Kim
Division of Vascular Surgery
Samsung Medical Center
Sungkyunkwan University School of Medicine
81 Irwon-ro, Gangnam-gu, Seoul 135-710, South Korea
Prof. S.-W. Cho
Department of Neurosurgery
Yonsei University College of Medicine
Seoul 120-750, South Korea

DOI: 10.1002/adfm.201500006

(e.g., methacrylate, aldehyde, or amine).[1,2] In particular, HA-methacrylate (HA-ME) synthesized by transesterification forms a hydrogel via photopolymerization using UV irradiation and photoinitiators.[6] Although this is a widely used HA crosslinking method, it generates free radicals that damage cells during their encapsulation.[7] Thus, photopolymerized HA hydrogel often causes adverse effects on the viability and proliferation of cells that are vulnerable to microenvironmental changes during crosslinking (e.g., stem/progenitor cells, primary cells).[7] In addition, HA-ME hydrogel does not exhibit sufficient tissue adhesion to allow minimally invasive cell transplantation and effective localization of transplanted cells in vivo.[8] In terms of its clinical application, the adhesive property of hydrogel would be advantageous for injection-free cell administration, as injection of hydrogel into certain organs (e.g., liver, heart) may induce tissue damage and hemorrhage.[9] Therefore, alternative HA crosslinking is required to produce highly biocompatible HA hydrogel with adhesive properties that render invasive injection procedures unnecessary.

Biomimetic strategies based on mussel-inspired chemistry can provide alternative and more efficient crosslinking methods that can overcome the limitations of current HA hydrogels. Polymerization of dopamine, a catecholamine containing adhesive motifs of *Mytilus edulis* foot protein (3,4-dihydroxy-L-phenylalanine and lysine), can be used for HA crosslinking to form 3D hydrogel. Oxidative conversion of the catechol group of dopamine to *o*-quinone is triggered by alkaline pH (>7.5), resulting in chemical crosslinking via the formation of catechol–catechol adducts.[10] This crosslinking principle has been employed to generate 3D hydrogel networks by conjugating catechol moieties to a variety of polymers (e.g., poly(ethylene glycol), chitosan, alginate, and HA) followed by oxidative crosslinking of the catechol groups.[11–15] This method does not require UV curing or the use of a photoinitiator and thus can provide a highly biocompatible 3D microenvironment within the hydrogel construct. Indeed, previous studies, including ours, report that HA-catechol (HA-CA) hydrogel is not cytotoxic or inflammatory either in vitro or in vivo.[14,15] Interestingly, catechol-modified hydrogels exhibit sufficient adhesion to stick onto diverse types of material surfaces including wet tissues,[12,14] which enables injection-free cell deposition onto defected tissues. The physicochemical and mechanical properties of these hydrogels can also be readily modulated by the degree of catechol conjugation.[16] Few studies, however, have demonstrated the advantages of catechol-functionalized hydrogel for in vivo therapeutic applications. In this study, we show that tissue-adhesive HA-CA hydrogel exhibits improved biocompatibility and can mediate minimally invasive cell therapy, resulting in enhanced therapeutic efficacy in diseased and defected animal models.

2. Results

2.1. Preparation and Characterization of HA-CA Hydrogel

HA-CA was synthesized by conjugating dopamine to the HA backbone (**Figure 1**a) via a carbodiimide coupling reaction using 1-ethyl-3-(3-dimethylaminopropyl) carbodiimide (EDC) and *N*-hydroxysulfosuccinimide (NHS) (Figure S1, Supporting Information). In this reaction, the molar ratio of dopamine to HA backbone was 1:1, and the conjugation efficiency of dopamine to the carboxyl group in the HA backbone was ≈4%–10%. The conjugation of dopamine to HA was confirmed by nuclear magnetic resonance (NMR), as indicated by the presence of catechol proton-specific peaks at around 7 ppm (Figure S1, Supporting Information). The conjugate was then crosslinked to form a hydrogel in the presence of an oxidation agent (sodium periodate; $NaIO_4$) at equal molar equivalents of $NaIO_4$ to catechol of the HA-CA conjugate under basic conditions (pH = 8) as previously described.[15] HA-CA conjugate is thought to be gel via formation of catechol–catechol adducts, reminiscent of monomer polymerization in melanin formation.[17] Upon gelation, the pregel solution turned brown immediately (Figure 1b) due to the oxidative conversion of the catechol moiety of the conjugate into *o*-quinone. HA-ME was synthesized by transesterification of methacrylate anhydride to the hydroxyl group of HA (Figure S1, Supporting Information), and hydrogel was formed via photopolymerization by exposure to UV light following addition of a photoinitiator (Irgacure 2959). HA-CA hydrogels with different degree of substitution (DS) of catechol (DS 4.5% and DS 8.8%) and HA-ME hydrogel with 9.8% methacrylate substitution (DS 9.8%) were used for the characterization.

The swelling properties of the HA-CA hydrogel (2%) were investigated by measuring changes in wet weight during 5 d of incubation under physiological conditions (i.e., in phosphate-buffered saline (PBS) at 37 °C) (Figure 1c). UV-crosslinked HA-ME hydrogel (2%), a widely used HA hydrogel system in biomedical applications, was used as a control throughout the study. There was no significant weight loss or structural deformation in either type of HA hydrogel (Figure 1c). Both hydrogels reached an equilibrium state of swelling after 2 d of incubation, which remained constant during the rest of the incubation period (Figure 1c). Notably, the HA-CA hydrogel exhibited a faster increase in wet weight and greater swelling capacity than the HA-ME hydrogel (181.2 ± 7.9% for HA-CA DS 4.5% and 124.3% ± 12.5% for HA-CA DS 8.8% vs 35.3% ± 9.0% for HA-ME DS 9.8% on day 5). When HA hydrogels were exposed to enzymatic degradation by hyaluronidase, the HA-CA hydrogel showed a faster rate of weight decrease compared to the HA-ME hydrogel (Figure 1d). After 2–4 h of incubation with the enzyme, the weight of the HA-CA hydrogel decreased to 50% of its initial value (2 h for the HA-CA DS 4.5% and 4 h for the HA-CA DS 8.8%), whereas it took 8 h for the HA-ME hydrogel (DS 9.8%) to undergo a 50% weight loss (Figure 1d). HA-CA and HA-ME hydrogels completely degraded ≈6–10 and 24 h after enzymatic treatment, respectively (Figure 1d).

Next, the rheological and viscoelastic properties of HA-CA hydrogel (2%) were investigated by dynamic mechanical analysis (**Figure 2**a). Storage modulus (G′) and loss modulus (G″) of the hydrogel were recorded in frequency sweep mode 10 min after the induction of gelation. In all frequency ranges tested (0.1 to 1 Hz), G′ was consistently higher than G″, indicating that the HA-CA hydrogel (DS 4.5% and DS 8.8%) was stable and behaved as a viscoelastic solid (Figure 2a). The average storage moduli measured at 1 Hz were 492 ± 32.7, 1321 ± 56.3, and 3443 ± 133.2 Pa for HA-CA DS 4.5%, HA-CA DS 8.8%,

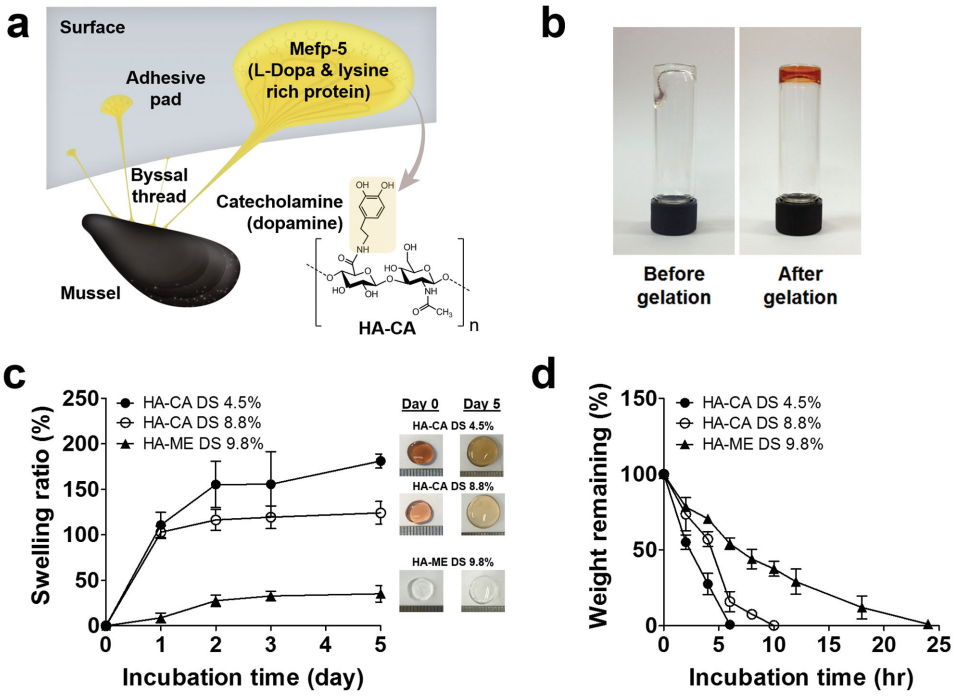

Figure 1. Physical characterization of HA-CA hydrogel. a) Schematic representation of engineered mussel-inspired HA hydrogel. The major component of the mussel adhesive protein, *Mytilus edulis* foot protein-5 (Mefp-5), is located in the adhesive pads. L-Dopa and lysine are the primary amino acids that give the protein adhesive property. Dopamine, a catecholamine containing both L-Dopa and lysine residues, was conjugated to HA for hydrogel formation. b) Gross view of HA-CA hydrogel before (left) and after (right) gelation. c) Swelling property of HA-CA and HA-ME hydrogels upon incubation at 37 °C ($n = 3$). d) Enzymatic degradation of HA hydrogels by hyaluronidase (100 U mL^{-1}). Remaining wet weights were measured at each time point ($n = 3$).

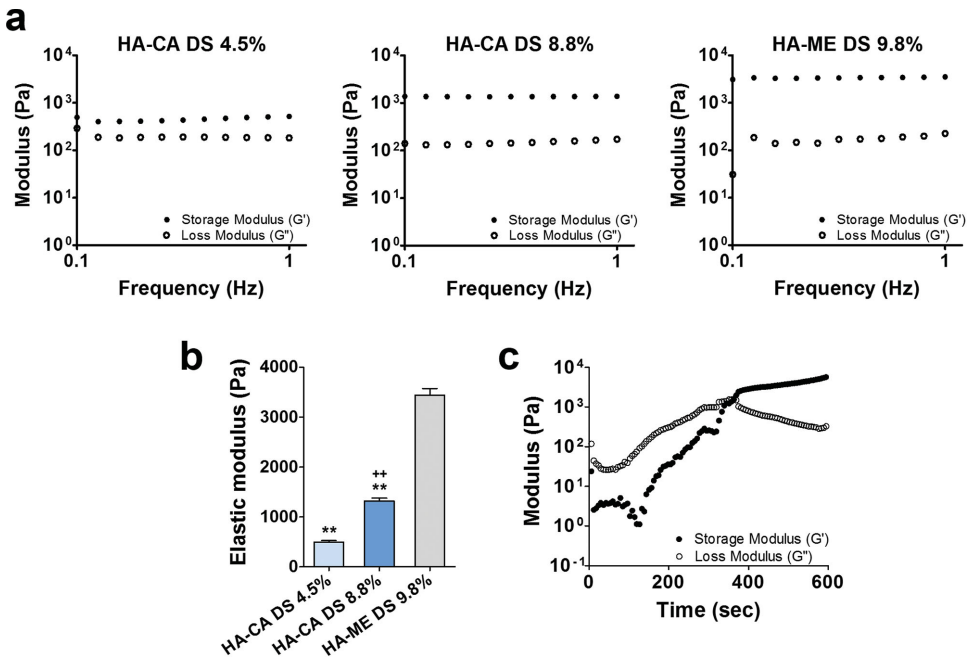

Figure 2. Rheometric analysis of HA-CA hydrogel. a) Rheometric analysis of HA-CA and HA-ME hydrogels in a frequency sweep mode. Black symbols are storage moduli G′, and white symbols are loss moduli G″. b) Average elastic modulus of HA-CA (DS 4.5% and DS 8.8%) and HA-ME hydrogel (DS 9.8%) at 1 Hz ($n = 3$, ++$p < 0.01$ vs HA-CA DS 4.5%, **$p < 0.01$ vs HA-ME DS 9.8%). c) Rheometric analysis in a time sweep mode to examine gelation kinetics of HA-CA hydrogel. The crossing time of G′ and G″ was considered as the gelation time.

and HA-ME DS 9.8% hydrogel (2%), respectively (Figure 2b), indicating that the HA-CA hydrogel was softer than the HA-ME hydrogel. Gelation kinetics were also evaluated in dynamic time sweep mode (Figure 2c). HA-CA formed a hydrogel around 6–7 min after gelation induction, as indicated by the crossover of G′ and G″ (Figure 2c).

2.2. Tissue Adhesive Property of HA-CA Hydrogel

The adhesion strength of HA hydrogel was measured by recording detachment stress of HA hydrogel from the tissue. The catechol group with a high binding affinity to diverse nucleophiles (e.g., amines, thiol, and imidazole) in HA-CA hydrogel can be anchored to peptides and proteins on tissue surface, which may provide a potential mechanism of tissue adhesion of HA-CA hydrogel (**Figure 3**a).[18,19] To cross-compare the adhesion properties of the HA-CA and HA-ME hydrogels prepared by different crosslinking chemistries, the HA-CA and HA-ME hydrogels with the similar degree of functional group substitution were included for the adhesion test (HA-CA DS 8.8% vs HA-ME DS 9.8%). Universal test machine (UTM) analysis for measuring adhesion strength of HA hydrogel to tissue (Figure 3b) [12] revealed that the adhesion strength of HA-CA hydrogel (DS 4.5%: 0.804 ± 0.079 kPa and DS 8.8%: 1.356 ± 0.084 kPa) to liver tissue was significantly higher than that of HA-ME hydrogel (DS 9.8%: 0.187 ± 0.057 kPa) (Figure 3c,d), demonstrating that only HA-CA hydrogel is adhesive enough to stick onto the surface of tissue with stability. The adhesion strength of HA-CA hydrogel to liver tissue was increased in proportion to catechol substitution (Figure 3c,d), confirming that the tissue adhesion strength of HA-CA hydrogel is largely dependent on the degree of catechol substitution to HA.

The interfacial fracture energy of adhesive HA-CA hydrogel was much larger than that of nonadhesive HA-ME hydrogel. As shown in Figure 3c, the fracture at the interface between HA-CA hydrogel (DS 8.8%) and liver tissue occurs about 1.5 mm of extension. The intrinsic mechanical property of liver tissue is too weak and thus the liver tissue is likely to undergo fracture of the liver tissue itself before occurring the fracture at the interface of the HA-CA hydrogel and liver tissue. Nevertheless, the interfacial fracture energy of HA-CA hydrogels (DS 8.8%: 1.1 J m^{-2} and DS 4.5%: 0.59 J m^{-2}) was calculated to be much greater than that of nonadhesive HA-ME hydrogel (DS 9.8%: 0.05 J m^{-2}).

2.3. Improved Viability and Hepatic Function of Hepatocytes in HA-CA Hydrogel

To test the applicability of adhesive HA-CA hydrogel for liver tissue engineering, we first investigated the viability and hepatic function of human hepatocytes (hHEPs) cultured in HA-CA hydrogel. Primary hepatocytes easily lose their viability and functionality after isolation, especially as single cells.[20] Thus, basic fibroblast growth factor (bFGF; 1 µg in 100 µL hydrogel), a mitogenic growth factor, was incorporated into the hydrogel to increase the viability of hHEPs during their culture. hHEPs encapsulated in HA-CA hydrogel showed greater viability than cells in HA-ME hydrogel at all time points (70.9% ± 2.5% for HA-CA and 52.2% ± 2.2% for HA-ME on day 14) (**Figure 4**a,b). Incorporation of bFGF into the HA-CA hydrogel further

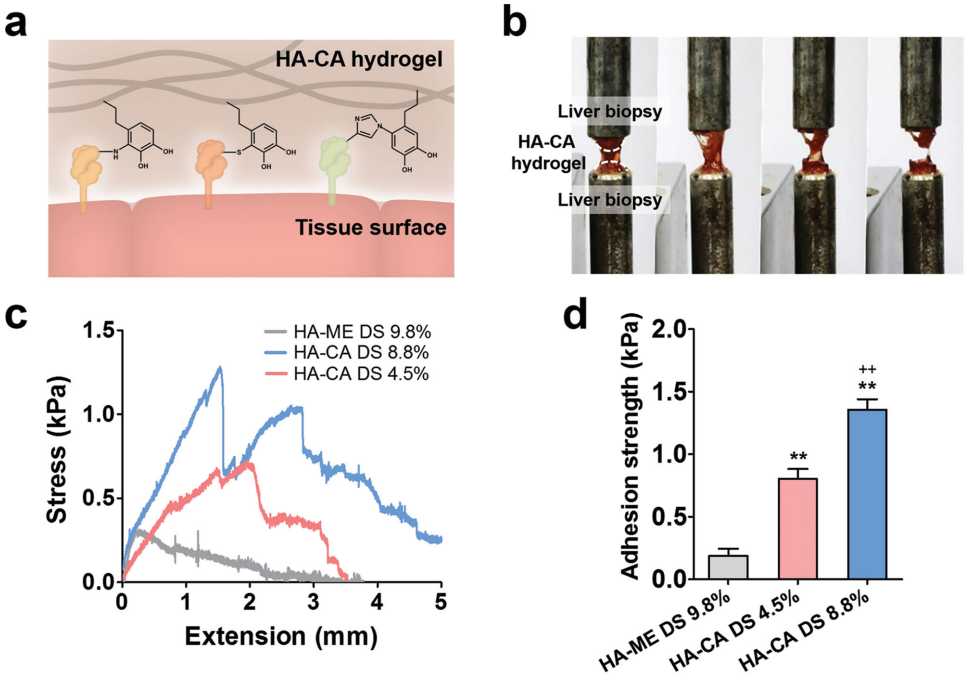

Figure 3. Tissue adhesion strength of HA-CA hydrogel. a) Schematic illustration showing a potential mechanism of the tissue adhesion of HA-CA hydrogel. b) The gross view images of the adhesion strength measurement of HA-CA hydrogel to liver tissue using UTM. c) Adhesion strength of HA-CA hydrogel (DS 4.5% and DS 8.8%) to rat liver tissue was compared with HA-ME hydrogel (DS 9.8%) using UTM ($n = 3$). d) Average adhesion strength of HA-CA and HA-ME hydrogel to rat liver tissue ($n = 3$, $^{**}p < 0.01$ vs HA-ME DS 9.8%, $^{++}p < 0.01$ vs HA-CA DS 4.5%).

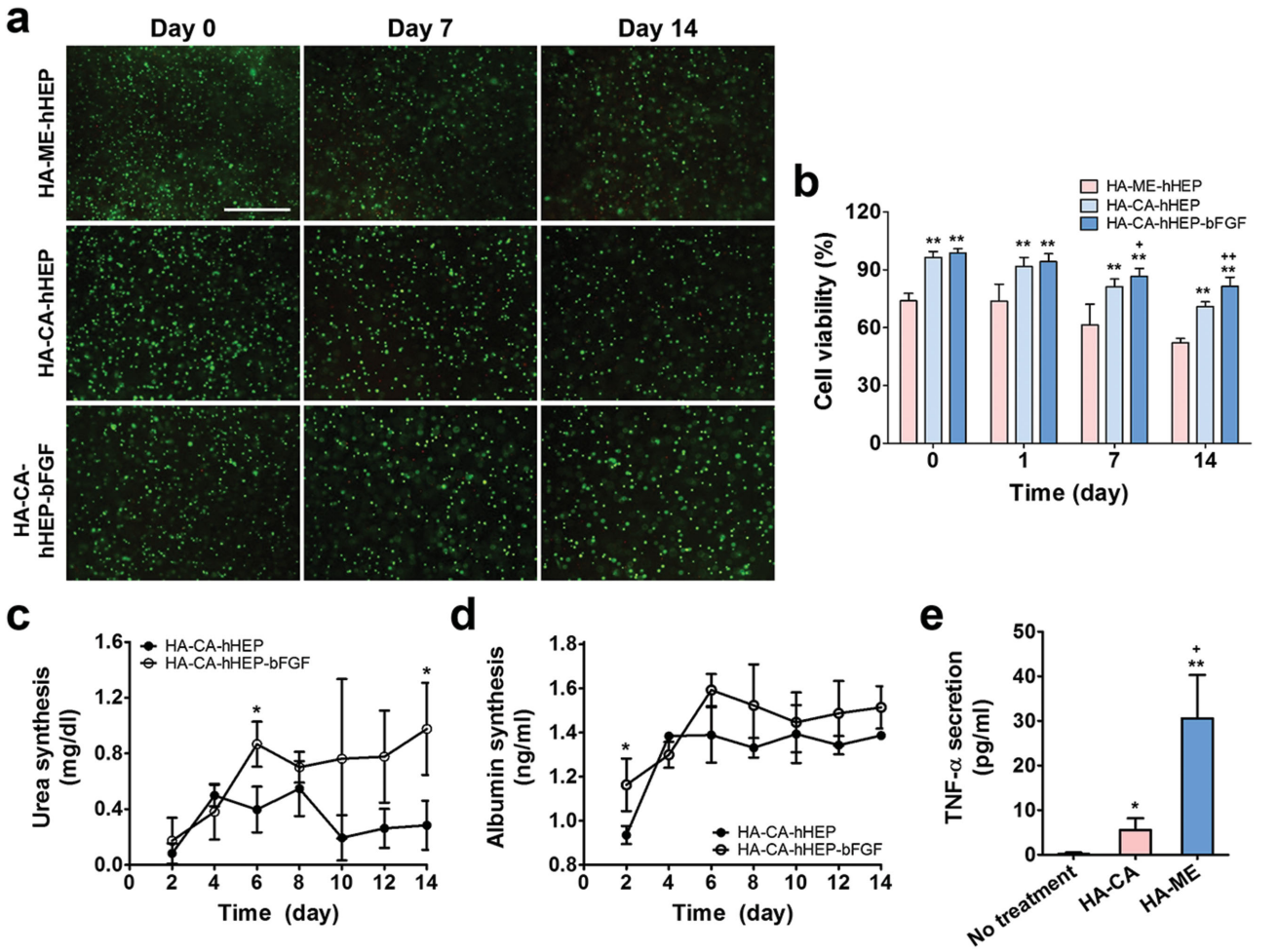

Figure 4. Maintenance of functional hepatocytes in HA-CA hydrogel. a) Live/Dead staining of human hepatocytes encapsulated in HA-CA hydrogel with or without bFGF and HA-ME hydrogel on day 0, 7, and 14. Scale bar = 1 mm. b) Viability of human hepatocytes cultured in HA-CA hydrogel (with or without bFGF) and HA-ME hydrogel ($n = 6$, $^{**}p < 0.01$ vs HA-ME-hHEP group, $^{+}p < 0.05$ and $^{++}p < 0.01$ vs HA-CA-hHEP group). Quantification of c) urea and d) albumin synthesized from human hepatocytes cultured in HA-CA hydrogel with or without bFGF ($n = 3$, $^{*}p < 0.05$ vs HA-CA-hHEP group). e) ELISA quantification of TNF-α secreted from RAW 264.7 cells in the presence of HA-CA or HA-ME hydrogel ($^{*}p < 0.05$ and $^{**}p < 0.01$ vs no treatment group, $^{+}p < 0.05$ vs HA-CA group).

improved the viability of hepatocytes after 14 d of encapsulation (81.4% ± 4.7%) (Figure 4a,b). Hepatocyte-specific functions, such as urea and albumin synthesis, were also well maintained or improved in hHEPs cultured in HA-CA hydrogel with addition of bFGF (Figure 4c,d).

HA-CA hydrogel was also tested for the 3D culture of primary mouse hepatocytes (mHEPs) (Figure S2, Supporting Information). Live/Dead staining revealed that the overall viability of mHEPs was low and decreased across culture days, but the viability of mHEPs encapsulated in HA-CA hydrogel with bFGF was higher at all time points compared with those without bFGF incorporation (Figure S2a,b, Supporting Information). Urea synthesis, as an indicator of hepatocyte function, was significantly greater in mHEPs encapsulated in HA-CA hydrogel with bFGF than in those without bFGF (Figure S2c, Supporting Information). Consistent with the urea synthesis results, significantly higher expression of albumin was found in encapsulated mHEPs with bFGF than in those without bFGF (Figure S2d, Supporting Information). Although not statistically significant, the expression of other hepatic genes, including cholesterol 7 alpha-hydroxylase (CYP7A1), glucose-6-phosphatase 3 (G6PC3), and hepatocyte nuclear factor 4 alpha (HNF-4α), was also upregulated in the presence of bFGF (Figure S2d, Supporting Information). Collectively, these results indicate that HA-CA hydrogel with incorporated bFGF aids in retaining the viability, functionality, and phenotype of primary hepatocytes in 3D culture.

To determine the immune-stimulating effect of HA hydrogel, tumor necrosis factor-α (TNF-α) secretion from RAW 264.7 macrophages in the presence of hydrogel was measured by enzyme-linked immunosorbent assay (ELISA). TNF-α secretion from cells cultured with HA-CA hydrogel (5.54 ± 2.64 pg mL^{-1}) was slightly increased relative to the negative control (0.18 ± 0.31 pg mL^{-1} with no hydrogel) but markedly lower than that from cells cultured with HA-ME hydrogel (30.54 ± 9.75 pg mL^{-1}) (Figure 4e). In vivo biocompatibility of the HA hydrogel was investigated by transplanting the hydrogel into the subcutaneous space of mice followed by histological

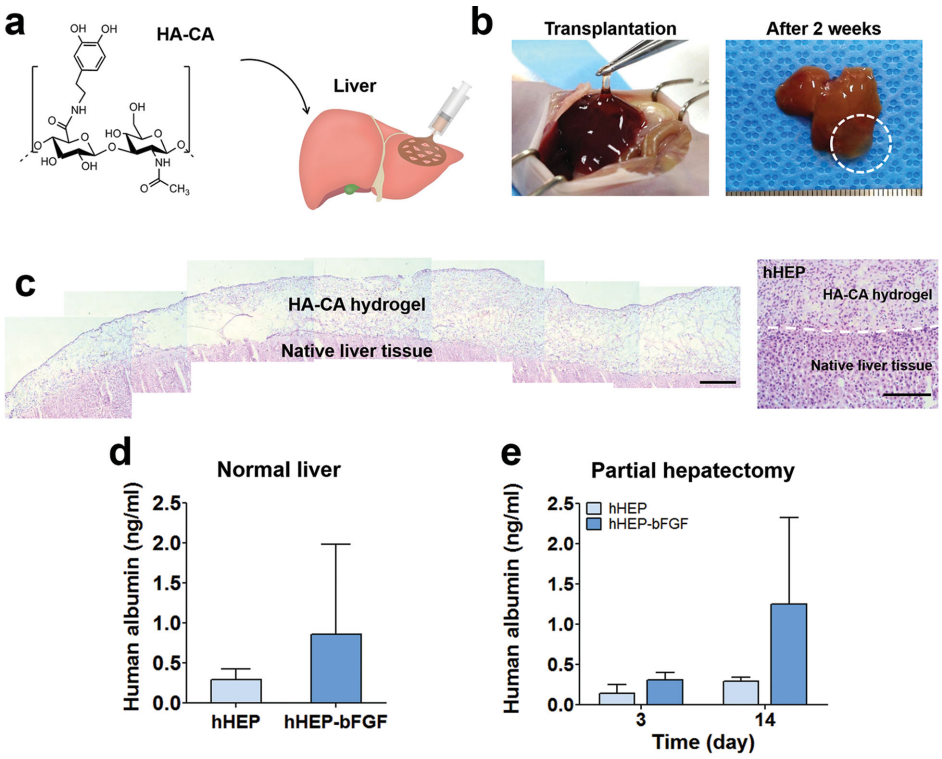

Figure 5. Injection-free transplantation of hepatocytes to the liver using adhesive HA-CA hydrogel. a) Schematic illustration of HA-CA hydrogel painting on liver lobes. b) Gross view of sticky HA-CA hydrogel immediately (left) and 2 weeks (right) after transplantation. c) H&E staining of HA-CA hydrogel with human hepatocytes painted on the surface of liver tissue (left) and enlarged view of the adhering region between HA-CA hydrogel and the surface of liver tissue (right). Scale bar = 1 mm (left) and 400 μm (right). The level of human albumin in blood serum was calculated in d) normal mice 3 d after transplantation ($n = 3$) and e) partial hepatectomy mice 3 and 14 d after transplantation ($n = 3$).

analysis. No apparent deformation or differences in the wet weight of either hydrogel were noted during 56 d of transplantation (Figure S3a,b, Supporting Information). Hematoxylin & eosin (H&E) staining of hydrogel constructs retrieved at several time points (days 3, 14, 28, and 56) indicated no infiltration of inflammatory cells into the hydrogels (Figure S3c, Supporting Information). All mice survived the initial operation and subsequent 56 d transplantation period without any abnormal behavior or physiological changes, and their body weights increased over the period within a normal range (Figure S3d, Supporting Information).

2.4. Injection-Free Transplantation of Hepatocytes onto the Liver Using Adhesive HA-CA Hydrogel

Finally, HA-CA hydrogel was tested for the injection-free transplantation of hHEPs (**Figure 5**a). hHEPs were transplanted onto liver tissue in an injection-free manner by painting the HA-CA pregel solution containing hHEPs on top of the liver lobe of athymic mice (Figure 5b). After ≈5–6 min of gelation, the sticky gel solution tightly bound to the liver lobe, and the formed gel remained attached 2 weeks after transplantation (Figure 5b). H&E staining of the hydrogel construct attached to the liver tissue 2 weeks after transplantation showed that the painted hydrogel tightly adhered to the surface of the tissue, and transplanted hHEPs were evenly distributed throughout the HA-CA hydrogel construct (Figure 5c). Interestingly, human albumin was detected in mouse serum 3 d after hHEP transplantation, indicating the survival and retained hepatic function of transplanted hHEPs (Figure 5d). Although it did not reach statistical significance, the level of human albumin was higher in hHEPs transplanted with bFGF compared to the cells without bFGF (Figure 5d). When hHEPs were similarly transplanted using HA-CA hydrogel onto the liver lobe of mice with partial hepatectomy,[21] human albumin was detected in mouse blood serum up to 2 weeks after transplantation (Figure 5e).

2.5. Enhanced Viability and Paracrine Ability of hADSCs in HA-CA Hydrogel

Cytotoxicity of HA hydrogels to human adipose-derived stem cells (hADSCs) was assessed by the Live/Dead assay. Immediately after encapsulation, the majority of cells were viable in both types of hydrogel (**Figure 6**a). hADSCs encapsulated in the HA-CA hydrogel exhibited highly elongated and spreading morphology and remained viable for 2 weeks (Figure 6a). By contrast, the viability of hADSCs encapsulated in the HA-ME hydrogel gradually declined over the 2 weeks culture period, and elongated cellular morphology was not observed (Figure 6a), suggesting that the HA-CA hydrogel provides a more favorable microenvironment for cells than the HA-ME hydrogel. Quantitative real-time polymerase chain reaction

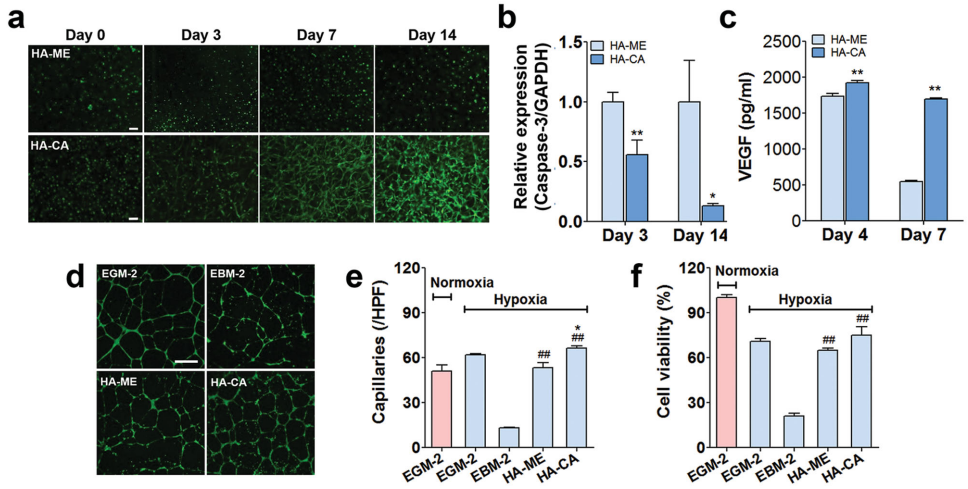

Figure 6. Enhanced viability and paracrine secretion of hADSCs in HA-CA hydrogel. a) Live/Dead staining of hADSCs encapsulated in HA-CA or HA-ME hydrogel (green: live, red: dead). Scale bar = 200 μm. b) Comparison of apoptotic marker gene expression (caspase-3) in hADSCs cultured in HA-CA and HA-ME hydrogels by qRT-PCR (*$p < 0.05$ and **$p < 0.01$ vs HA-ME group). c) ELISA quantification of VEGF secreted from hADSCs encapsulated in HA hydrogels (**$p < 0.01$ vs HA-ME group). d–f) Evaluation of capillary tube formation by HUVECs on Matrigel and the viability of HUVECs cultured in conditioned medium from hADSCs encapsulated in HA hydrogels. d) Calcein AM staining of capillaries formed by HUVECs after overnight incubation under hypoxia (1% oxygen) with EGM-2, EBM-2, or conditioned medium from hADSC culture in HA hydrogels. Scale bar = 500 μm. e) The number of capillaries formed by HUVECs in response to conditioned medium from HA-CA hydrogel cultures and other media (*$p < 0.05$ vs HA-ME group, ##$p < 0.01$ vs EBM-2 group). f) MTT assay to determine the viability of HUVECs cultured in hypoxic conditions (##$p < 0.01$ vs EBM-2 group).

(qRT-PCR) analysis showed that gene expression of caspase-3, a pro-apoptotic factor, was significantly lower in hADSCs encapsulated with HA-CA hydrogel compared to those encapsulated with HA-ME hydrogel on day 3 of culture (Figure 6b). The difference in caspase-3 expression between HA-CA and HA-ME hydrogel groups became more apparent by day 14. This finding also indicates that the HA-CA hydrogel enhances the viability of hADSCs. The substitution degree of catechol functional group to HA (DS 4.5% and DS 8.8%) did not affect the viability and spreading of hADSCs cultured in the HA hydrogel (Figure S4a, Supporting Information).

The use of ADSCs is promising for therapeutic angiogenesis because ADSCs can secrete several angiogenic paracrine signals, such as vascular endothelial growth factor (VEGF). Therefore, the secretion of VEGF from hADSCs encapsulated in HA-CA hydrogel was measured to assess the potential application of the HA-CA hydrogel system in the treatment of ischemic diseases. After 4 d of hADSC culture in HA hydrogel, the level of secreted VEGF in the HA-CA group was significantly higher than that in the HA-ME group (Figure 6c). Interestingly, the level of released VEGF only slightly decreased in the HA-CA group from day 4 to 7 (1925.1 ± 27.9 pg mL^{-1} at day 4 and 1696.0 ± 35.5 pg mL^{-1} at day 7), whereas it was significantly reduced in the HA-ME group to a level threefold lower than that in the HA-CA group (1737.4 ± 35.5 pg/ml at day 4 and 551.8 ± 10.3 pg mL^{-1} at day 7). This observation may be explained by the increased viability and reduced apoptosis of hADSCs observed in HA-CA hydrogel. VEGF secretion from hADSCs in HA-CA hydrogel was not significantly affected by substitution degree of catechol group in HA-CA hydrogel (DS 4.5%: 1241.7 ± 161.8 pg mL^{-1}, DS 8.8%: 1299.2 ± 41.5 pg mL^{-1} at day 1 and DS 4.5%: 1654.6 ± 78.7 pg mL^{-1}, DS 8.8%: 1703.0 ± 21.2 pg mL^{-1} at day 4) (Figure S4b, Supporting Information).

Enhanced paracrine secretion from hADSCs encapsulated in HA-CA hydrogel was also evident in the capillary tube formation assay (Figure 6d,e). Human umbilical cord blood endothelial cells (HUVECs) were cultured on Matrigel under hypoxia (1% oxygen) with conditioned medium from the 3D culture of hADSCs in the hydrogel. HUVECs formed more extensive networks of capillary-like structures in the presence of conditioned medium from HA-CA-hADSCs than endothelial basal medium-2 (EBM-2) or conditioned medium from HA-ME-hADSCs (Figure 6d,e). Moreover, the viability of HUVECs cultured with conditioned medium from HA-CA-hADSCs was similar to that of cells cultured in endothelial growth medium-2 (EGM-2) and higher than that of cells cultured in EBM-2 or conditioned medium from HA-ME-hADSCs (Figure 6f). These results provide further evidence that HA-CA hydrogel provides higher viability and enhanced angiogenic efficacy of hADSCs compared to HA-ME hydrogel.

2.6. Injection-Free Transplantation of hADSCs onto the Heart Using Adhesive HA-CA Hydrogel

As another application of the adhesive property of HA-CA hydrogel, hADSCs encapsulated in HA-CA hydrogel were transplanted onto the ischemic myocardium of a rat heart without injection (**Figure 7**a). Myocardial infarction was induced in athymic rats by ligation of the left coronary artery.[22] Pregel solution of HA-CA containing hADSCs was painted directly onto the infarcted region of beating hearts (Figure 7b). The HA-CA hydrogel showed higher adhesive strength to heart tissue compared with HA-ME hydrogel (Figure 7c), indicating that only HA-CA hydrogel was capable of sticking onto the surface of heart tissue with stability. The adhesion strength of HA-CA and HA-ME hydrogels was 47.61 ± 36.12

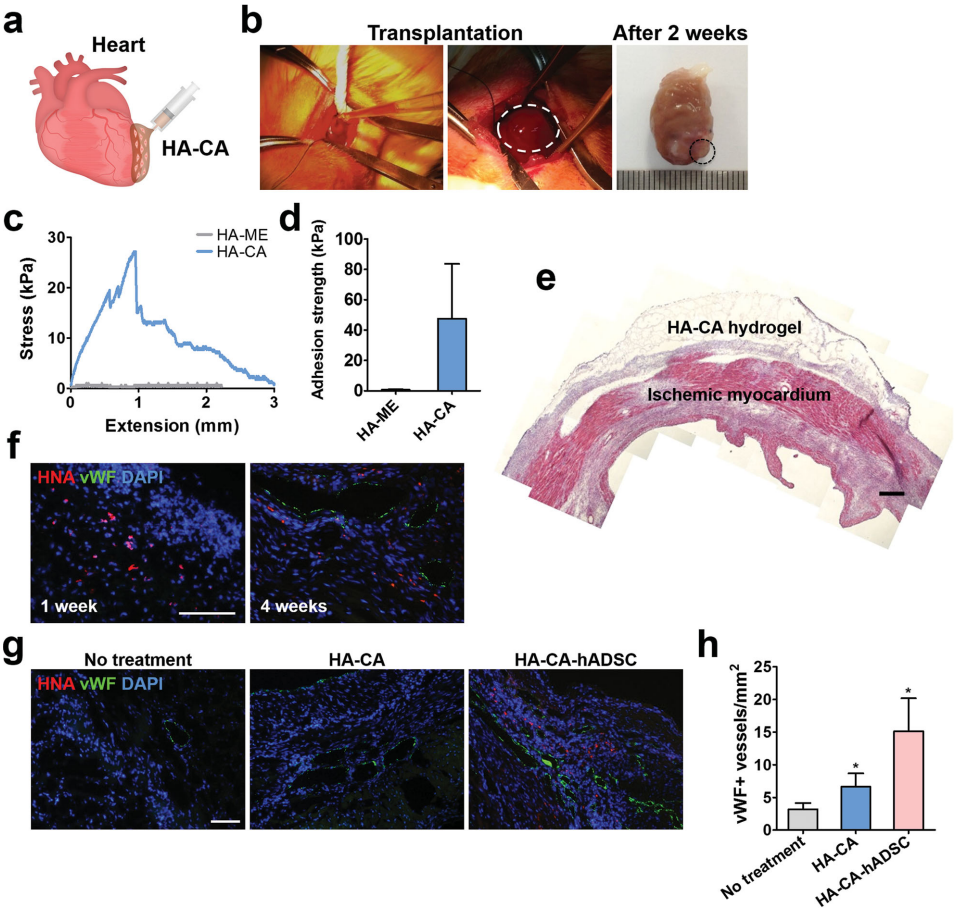

Figure 7. Angiogenesis induced by injection-free transplantation of hADSCs using adhesive HA-CA hydrogel onto the ischemic myocardium. a) Schematic illustration of HA-CA hydrogel painting onto the surface of the heart. b) Gross view of the sticky HA-CA hydrogel immediately (left, middle) and 2 weeks after (right) transplantation. c) Adhesion strength of the HA-CA hydrogel on the surface of rat heart tissue was evaluated by UTM ($n = 3$). d) Average adhesion strength of HA-CA and HA-ME hydrogel to rat heart tissue ($n = 3$). e) H&E staining of HA-CA hydrogel-painted ischemic myocardium. Scale bar = 1 mm. Dual immunofluorescence staining of HNA (red) for hADSCs and vWF (green) for blood vessels to trace f) transplanted hADSCs that migrated from the hydrogel into the infarcted site of myocardium 1 and 4 weeks post-treatment and to confirm g) blood vessel formation in infarcted area 4 weeks post-treatment (no treatment, HA-CA, and HA-CA-hADSC groups). Scale bar = 200 μm. h) Quantification of vWF-positive vessels in the infarcted myocardium 4 weeks after treatment ($n = \approx 5–10$, $^*p < 0.05$ vs no treatment group).

and 0.64 ± 0.35 kPa, respectively (Figure 7d). The difference in adhesion strength of HA-CA hydrogel between liver and heart tissue (Figures 3c and 7c) was probably due to different surface moieties for catechol binding and differences in the mechanical properties of the two tissues. The HA-CA hydrogel remained intact 2 weeks after transplantation (Figure 7b) and formed a tight connection with the heart tissue as confirmed by H&E staining (Figure 7e).

The transplanted hADSCs migrated from the HA-CA hydrogel into the infarcted region 1 week after transplantation as indicated by immunofluorescent staining of human nuclear antigen (HNA) marker (Figure 7f). hADSCs were observed deeper inside the ischemic myocardium 4 weeks after transplantation (Figure 7f). In addition, the number of blood vessels (von Willebrand factor (vWF)-positive vessels) was markedly increased by hADSC transplantation using HA-CA hydrogel compared to no treatment or HA-CA hydrogel alone conditions (Figure 7g,h) due to the paracrine effect of transplanted hADSCs. These results suggest that injection-free transplantation of hADSCs using adhesive HA-CA hydrogel enhances angiogenesis in the ischemic myocardium.

3. Discussion

Our study suggests that a bioinspired HA hydrogel overcomes the limitations of conventional photopolymerized HA hydrogel systems for cell therapy and tissue reconstruction. hHEPs and hADSCs cultured in HA-CA hydrogel showed enhanced viability and reduced apoptosis compared to cells in HA-ME hydrogel. The poorer viability of cells in photopolymerized HA-ME hydrogel may be explained by crosslinking involving the use of a photoinitiator and UV irradiation, causing the production of free radicals.[7] Soluble components eluted from HA-CA hydrogel seemed to be less immunogenic compared with the radicals and remaining photoinitiators released from HA-ME hydrogel, suggesting that HA-CA hydrogel may only marginally activate immune lineage cells. Thus, as HA-CA hydrogel may

not have significant immune-stimulating effects, it may therefore cause little irritation in vivo, indicating a reduced immunogenicity and superior biocompatibility of HA-CA hydrogel compared with photopolymerized HA hydrogel. Accordingly, HA-CA hydrogel enhanced the viability and paracrine secretion of hADSCs, leading to marked improvements in the angiogenic efficacy of transplanted hADSCs in ischemic heart muscle for therapeutic angiogenesis.

Catechol-modified HA hydrogel can provide highly tunable, more favorable biophysical and mechanical microenvironments for effective cell therapy compared with HA-ME hydrogel. We found that the gelation time of the HA-CA conjugate can be readily modulated by controlling the amount of oxidizing agent and adjusting the pH condition (i.e., NaOH concentration) for several seconds to more than 30 min.[15] In the present study, the formation of HA-CA hydrogel was adjusted to a gelation time of around ≈6–7 min, which can provide a time frame suitable for the handling of cell-containing hydrogel solution and its administration for cell therapy. Crosslinking density seemed to be lower in the HA-CA hydrogel compared to the HA-ME hydrogel because the conjugation of catechol to HA (≈4%–10%) is generally lower than that of methacrylate (≈10%–20%) under the same synthesis conditions. This leads to greater water uptake capacity and swelling due to efficient diffusion of aqueous solution into the hydrogel interior. This physical characteristic of HA-CA hydrogel may facilitate diffusion of nutrients and metabolites required for the activity and function of encapsulated cells.[23] The mechanical properties of HA-CA hydrogel could be tuned by adjusting the ratio of catechol conjugation to the HA backbone during its synthesis and changing the concentration of conjugate solution for gelation.[3,16,24] HA-CA hydrogel was found to be softer than HA-ME hydrogel as indicated by a lower modulus, which enhances the spreading and migration of encapsulated cells. HA-CA hydrogel also possesses microporous, interconnected internal structures,[15] which can contribute to creating a favorable 3D microenvironment for the adhesion, migration, and proliferation of encapsulated cells in the hydrogel construct.

In addition, catechol-modified HA hydrogel can easily and efficiently incorporate various growth factors and bioactive molecules and thereby have synergistic effects on tissue regeneration following cell transplantation. Proteins or peptides can efficiently bind to the catechol group of the HA-CA hydrogel due to the high affinity of nucleophiles such as amine, thiol, and imidazole to catechol moieties.[13,18,19,25] Our previous study shows that bFGF can be incorporated and tightly bound into a catechol-modified alginate hydrogel.[13] bFGF was not released from the hydrogel construct during a 2 weeks incubation under physiological conditions (in PBS at 37 °C), indicating that almost all loaded bFGF (≈100%) was tightly conjugated to the catechol group of the hydrogel.[13] It is thought that loaded growth factors and peptides are chemically conjugated to the catechol moiety of the hydrogel rather than being physically entrapped in the hydrogel.[13,18] Thus, growth factors or peptides incorporated into catechol-functionalized hydrogels can affect cells in the hydrogel constructs over an extended time period without a loss of loaded biomolecules. Primary hepatocytes easily lose their phenotype, viability, and hepatocyte-specific functions during in vitro culture and after in vivo transplantation. Incorporation of bFGF into the HA-CA hydrogel, however, improved the viability and hepatic function of hepatocytes both in vitro and in vivo (Figures 4 and 5).

The tissue adhesiveness of HA-CA hydrogel, which is the most interesting feature of this mussel-inspired hydrogel, was tested by way of its injection-free cell transplantation onto liver and heart tissue. The high affinity of oxidized catechol in HA-CA hydrogel to diverse nucleophiles (e.g., amines, thiol, and imidazole) may induce the strong binding of peptides and proteins on tissue surface to HA-CA hydrogel, improving tissue adhesion of HA-CA hydrogel (Figure 3a). The adhesive property of HA-CA hydrogel can be tuned and optimized for specific types of tissues by adjusting degree of catechol substitution to HA backbone (Figure 3c,d). We confirmed that HA-CA hydrogel adheres to liver and heart tissue, which in turn facilitates the direct engraftment of cell-encapsulating hydrogels onto the surface of these organs without injection or invasive procedures. A recent study demonstrates that catechol-modified hydrogels (alginate-catechol and HA-CA) showed strong adhesion to wet and dynamic environments and could simply be painted onto atherosclerotic plaques formed on the endothelium of blood vessels to serve as a steroid-eluting adhesive depot.[14] Although the size of HA-CA hydrogel was decreased after deposition on the liver and cardiac tissues, we observed stable and tight adhesion of the remaining HA-CA hydrogels onto those tissues up to 2–4 weeks after cell transplantation (Figures 5 and 7), ensuring low possibility of rapid disappearance and detachment from the tissues after deposition. In future studies, we need to check the in vivo adhesion stability and degradation of HA-CA hydrogel in a much longer time period. Considering the improved biocompatibility of catechol-functionalized hydrogels, they are expected to be able to deliver therapeutic cells at desired sites while maintaining cell viability and functionality, ultimately providing an easy and effective strategy for cell therapy. These aspects of our HA-CA hydrogel would be more important for clinical setting of cell transplantation.

Degradation mechanism of HA-CA hydrogel needs to be elucidated in future studies. It was previously reported that $NaIO_4$ induces polysaccharide degradation via opening of sugar rings.[26] Purcell et al. showed decreased molecular weight of HA in the presence of $NaIO_4$ in a concentration-dependent manner. They observed the degradation of HA from 390 to 76 kDa by the treatment of $NaIO_4$ at 1:4 molar ratio of $NaIO_4$:HA.[26] Therefore, the opening of sugar rings by $NaIO_4$ may render the structure of HA hydrogel more flexible and hydrolytically labile, which may lead to a faster mass loss of HA-CA hydrogel than HA-ME hydrogel as shown in Figure 1d. In our study, in order to induce catechol-based oxidative crosslinking, we added $NaIO_4$ at 1:10–14 molar ratio of $NaIO_4$:HA, which was much less than the amount of $NaIO_4$ used in the previous study. Thus, the effect of $NaIO_4$ on the mass loss of HA hydrogel may not be significant in our HA-CA hydrogel system. The potential mechanism of HA-CA degradation caused by $NaIO_4$ should be further examined in future studies.

In the current study, tissue-adhesive HA-CA hydrogel was capable of mediating hepatocyte transplantation to the liver in a minimally invasive manner without the need for injection. The direct infusion of hepatocytes into the hepatic portal vein is a typical route for hepatocyte transplantation to the liver, but

this procedure does not permit the localization of transplanted cells with high viability.[27] Rather, only ≈2%–5% of transplanted hepatocytes were found to be viable and functional after typical administration through the hepatic portal vein.[27] Thus, a large number of the cells must be administered to achieve an adequate level of therapeutic efficacy, but this often leads to complications caused by portal vein thrombosis.[27] Using HA-CA hydrogel, however, we simply applied the hydrogel containing human hepatocytes onto the largest liver lobe of athymic mice (Figure 5b). This procedure led to the direct transplantation of a relatively large number of human hepatocytes (1.0×10^6 cells) to the liver without invasive injection procedures that may cause tissue damage or hemorrhage. The HA-CA hydrogel construct remained tightly bound to the surface of the liver for up to 2 weeks and supported the viability and function (i.e., albumin secretion) of transplanted hepatocytes even on a liver with partial hepatectomy (Figure 5c–e). Long-term transplantation studies are required to determine whether transplanted cells migrate and integrate into the liver and whether the hydrogel supports the long-term efficacy of transplanted hepatocytes with structural stability. In future studies, diverse cell types such as hepatocyte spheroids, oval cells, or stem cell-derived hepatocyte-like cells could be transplanted onto the liver through this adhesive hydrogel-based method.[28]

Similar to the liver, most current techniques of cell transplantation to the heart with myocardial infarction involve invasive procedures such as direct injection of cells or materials into the infarcted site or infusion into the coronary artery.[29] Intramuscular cell administration into cardiac muscle and the attachment of cell-seeded patches require injection or suturing, which might damage the tissues and induce bleeding. Intracoronary artery infusion also limits the number of cells that can be transplanted.[30] Hence, it would be therapeutically valuable if cells could be successfully transplanted into ischemic myocardium using adhesive hydrogel without any direct invasive procedures. In the present study, the HA-CA hydrogel was deposited on beating hearts, where it formed a tissue-like layer tightly bound onto the ischemic myocardium (Figure 7b,e). Furthermore, the migration and engraftment of hADSCs from the attached hydrogel into the ischemic myocardium enhanced angiogenesis in ischemic tissue (Figure 7f,g). As the angiogenic efficacy of transplanted hADSCs was followed for only 4 weeks after cell transplantation, further studies are required to monitor the efficacy of cell therapy and the stability of the hydrogel on the heart during long-term transplantation. Future studies should also perform functional evaluations of infarcted hearts using echocardiography or magnetic resonance imaging analysis to confirm the therapeutic efficacy of adhesive hydrogel-mediated cell transplantation.

HA-CA hydrogel can provide the unique advantages for stem cell therapy over other catechol-functionalized hydrogels prepared from other polymers including alginate, chitosan, and poly(ethylene glycol). Catechol-functionalized hydrogels have a common feature of highly adhesive properties, which makes them suitable for tissue adhesive and glue as well as cell and drug carriers. However, HA-CA hydrogel may be the most suitable biomaterial for stem cell therapy because HA has cellular adhesion motifs for binding of diverse types of stem cells including embryonic stem cells, neural stem cells, and mesenchymal stem cells.[2,5,31,32] The cell binding to HA matrix is known to be crucial for stem cell survival and their functions.[1,33] Several studies have indeed reported the applicability of HA-based hydrogels for enhancing survival, proliferation, and differentiation of these stem cells.[2,5,31] The enhanced cellular interaction for stem cell survival and functions would be a unique feature of HA-CA hydrogel distinct from other catechol-functionalized hydrogels. Therefore, HA-CA hydrogel enables more effective stem cell transplantation with enhanced therapeutic efficacy through its tissue adhesive properties and enhanced cellular interaction.

4. Conclusions

In summary, we demonstrated the feasibility of bioinspired HA-CA hydrogel for effective, minimally invasive cell therapy in defected and diseased animal models. HA-CA hydrogel was shown to be more biocompatible and tissue adhesive compared with photopolymerized HA hydrogel. The adhesiveness of HA-CA hydrogel allowed the cell-containing hydrogel to simply be painted directly onto tissues, even in wet or beating states. The hydrogel was easily deposited onto liver and heart surfaces and adhered well to the tissues even after a month. The improved biocompatibility of HA-CA hydrogel enhanced the therapeutic and regenerative capacity of transplanted cells for angiogenesis and hepatic function. Consequently, the biocompatible, tissue-adhesive HA-CA hydrogel is expected to provide a novel method for highly effective but minimally invasive cell therapy.

Supporting Information

Supporting Information is available from the Wiley Online Library or from the author.

Acknowledgements

J.S., J.S.L., and C.L. contributed equally to this work. This work was supported by a grant (NRF-2010–0020409) from the National Research Foundation of Korea (NRF) and a grant (2009–0083522) from the Translational Research Center for Protein Function Control (TRCP) funded by the Ministry of Science, ICT, and Future Planning (MSIP), South Korea. This work was also supported by grants (HI13C1479 and HI14C1588) from the Korea Health Technology R&D Project funded by the Ministry of Health and Welfare, South Korea. This work was supported in part by the BK21 PLUS program. Jisoo Shin, Jung Seung Lee, and Hyun-Ji Park are fellowship awardee by BK21 PLUS program.

Received: January 1, 2015
Revised: April 15, 2015
Published online: May 15, 2015

[1] J. A. Burdick, G. D. Prestwich, *Adv. Mater.* **2011**, *23*, H41.
[2] S. Gerecht, J. A. Burdick, L. S. Ferreira, S. A. Townsend, R. Langer, G. Vunjak-Novakovic, *Proc. Natl. Acad. Sci. U.S.A.* **2007**, *104*, 11298.
[3] S. K. Seidlits, Z. Z. Khaing, R. R. Petersen, J. D. Nickels, J. E. Vanscoy, J. B. Shear, C. E. Schmidt, *Biomaterials* **2010**, *31*, 3930.

[4] K. Y. Lee, D. J. Mooney, *Chem. Rev.* **2001**, *101*, 1869.
[5] L. Bian, M. Guvendiren, R. L. Mauck, J. A. Burdick, *Proc. Natl. Acad. Sci. U.S.A.* **2013**, *110*, 10117.
[6] a) S. Khetan, M. Guvendiren, W. R. Legant, D. M. Cohen, C. S. Chen, J. A. Burdick, *Nat. Mater.* **2013**, *12*, 458; b) J. A. Burdick, C. Chung, X. Jia, M. A. Randolph, R. Langer, *Biomacromolecules* **2005**, *6*, 386.
[7] N. E. Fedorovich, M. H. Oudshoorn, D. van Geemen, W. E. Hennink, J. Alblas, W. J. Dhert, *Biomaterials* **2009**, *30*, 344.
[8] J. Baier Leach, K. A. Bivens, C. W. Patrick Jr., C. E. Schmidt, *Biotechnol. Bioeng.* **2003**, *82*, 578.
[9] a) S. Jiang, P. Li, Y. Yu, J. Liu, Z. Yang, *J. Biomech.* **2014**, *47*, 3344; b) S. Badaan, D. Petrisor, C. Kim, P. Mozer, D. Mazilu, L. Gruionu, A. Patriciu, K. Cleary, D. Stoianovici, *Int. J. Med. Robot. Comp.* **2011**, *7*, 138.
[10] H. Lee, S. M. Dellatore, W. M. Miller, P. B. Messersmith, *Science* **2007**, *318*, 426.
[11] B. P. Lee, J. L. Dalsin, P. B. Messersmith, *Biomacromolecules* **2002**, *3*, 1038.
[12] J. H. Ryu, Y. Lee, W. H. Kong, T. G. Kim, T. G. Park, H. Lee, *Biomacromolecules* **2011**, *12*, 2653.
[13] C. Lee, J. Shin, J. S. Lee, E. Byun, J. H. Ryu, S. H. Um, D. I. Kim, H. Lee, S. W. Cho, *Biomacromolecules* **2013**, *14*, 2004.
[14] C. J. Kastrup, M. Nahrendorf, J. L. Figueiredo, H. Lee, S. Kambhampati, T. Lee, S. W. Cho, R. Gorbatov, Y. Iwamoto, T. T. Dang, P. Dutta, J. H. Yeon, H. Cheng, C. D. Pritchard, A. J. Vegas, C. D. Siegel, S. MacDougall, M. Okonkwo, A. Thai, J. R. Stone, A. J. Coury, R. Weissleder, R. Langer, D. G. Anderson, *Proc. Natl. Acad. Sci. U.S.A.* **2012**, *109*, 21444.
[15] S. Hong, K. Yang, B. Kang, C. Lee, I. T. Song, E. Byun, K. I. Park, S. W. Cho, H. Lee, *Adv. Funct. Mater.* **2013**, *23*, 1774.
[16] D. G. Barrett, D. E. Fullenkamp, L. He, N. Holten-Andersen, K. Y. C. Lee, P. B. Messersmith, *Adv. Funct. Mater.* **2013**, *23*, 1111.
[17] B. P. Lee, P. B. Messersmith, J. N. Israelachvili, J. H. Waite, *Annu. Rev. Mater. Res.* **2011**, *41*, 99.
[18] H. Lee, J. Rho, P. B. Messersmith, *Adv. Mater.* **2009**, *21*, 431.
[19] a) K. Yang, J. S. Lee, J. Kim, Y. B. Lee, H. Shin, S. H. Um, J. B. Kim, K. I. Park, H. Lee, S. W. Cho, *Biomaterials* **2012**, *33*, 6952; b) E. Ko, K. Yang, J. Shin, S. W. Cho, *Biomacromolecules* **2013**, *14*, 3202.
[20] W. Zhang, L. Tucker-Kellogg, B. C. Narmada, L. Venkatraman, S. Chang, Y. Lu, N. Tan, J. K. White, R. Jia, S. S. Bhowmick, S. Shen, C. F. Dewey Jr., H. Yu, *Adv. Drug Delivery Rev.* **2010**, *62*, 814.
[21] C. Mitchell, H. Willenbring, *Nat. Protoc.* **2008**, *3*, 1167.
[22] K. S. Hong, K. H. Byun, J. Seo, H. J. Lee, J. J. Choi, K. S. Kim, Y. Choi, S. H. Moon, H. M. Chung, *Biotechnol. Lett.* **2014**, *36*, 859.
[23] P. J. Martens, S. J. Bryant, K. S. Anseth, *Biomacromolecules* **2003**, *4*, 283.
[24] D. Eng, M. Caplan, M. Preul, A. Panitch, *Acta. Biomater.* **2010**, *6*, 2407.
[25] Y. B. Lee, Y. M. Shin, J. H. Lee, I. Jun, J. K. Kang, J. C. Park, H. Shin, *Biomaterials* **2012**, *33*, 8343.
[26] B. P. Purcell, D. Lobb, M. B. Charati, S. M. Dorsey, R. J. Wade, K. N. Zellars, H. Doviak, S. Pettaway, C. B. Logdon, J. A. Shuman, *Nat. Mater.* **2014**, *13*, 653.
[27] K. Ohashi, F. Park, M. A. Kay, *J. Mol. Med.* **2001**, *79*, 617.
[28] J. S. Lee, S.-W. Cho, *Biotechnol. Bioprocess Eng.* **2012**, *17*, 427.
[29] N. Lang, M. J. Pereira, Y. Lee, I. Friehs, N. V. Vasilyev, E. N. Feins, K. Ablasser, E. D. O'Cearbhaill, C. Xu, A. Fabozzo, *Sci. Transl. Med.* **2014**, *6*, 218ra6.
[30] K. Suzuki, B. Murtuza, S. Fukushima, R. T. Smolenski, A. Varela-Carver, S. R. Coppen, M. H. Yacoub, *Circulation* **2004**, *110*, II225.
[31] Y. Liang, P. Walczak, J. W. Bulte, *Biomaterials* **2013**, *34*, 5521.
[32] G. Martino, S. Pluchino, *Nat. Rev. Neurosci.* **2006**, *7*, 395.
[33] H. J. Chung, T. G. Park, *Adv. Drug Delivery Rev.* **2007**, *59*, 249.